ELSEVIER

Thermochimica Acta 377 (2001) 159–172

thermochimica acta

www.elsevier.com/locate/tca

A new light driven spectrometer for the determination of complex heat capacities and conductivities by combination of effusivity and diffusivity measurements

Thomas Albrecht, Simon Armbruster, Brend Stühn, Kersten Vogel, Gert Strobl*

Fakultät für Physik, Albert-Ludwigs-Universität, Hermann-Herder-Str. 3, D-79104 Freiburg, Germany

Received 25 October 2000; received in revised form 3 February 2001; accepted 5 February 2001

Abstract

We describe the construction, performance and first application of a spectrometer for measurements of frequency-dependent complex thermal diffusivities and effusivities. Knowledge of these quantities enables the complex dynamic specific heat and the thermal conductivity to be calculated. The technique uses the properties of thermal waves initiated at the surface of plate-like samples by the absorption of light with an oscillating intensity. A registration of the resulting temperature oscillations in the absorbance layer at the upper surface of the sample yields the effusivity, an analogous measurement at the bottom gives the diffusivity. The detection of both amplitudes and phases of the signals leads to complex quantities. Measurements encompass a frequency range from 10^{-2} to 10^{2} Hz. The apparatus was used in a study of the reversible surface melting of poly(ethylene oxide). Both the magnitude and the characteristic time range of this process could be determined.

Keywords: Dynamic heat capacity; Thermal waves; Polymer melting

1. Introduction

Measurements of the dynamic heat capacity by modulation techniques have become a powerful tool for investigating the dynamics of thermally activated processes, e.g. the glass transition and the continuous melting in polymeric systems. Different experimental methods have been developed: temperature-modulated differential scanning calorimetry (TMDSC) [1–4], alternating current calorimetry (ACC) [5–7], temperature wave transmission spectroscopy (TTS) [8–10] and 3ω heat capacity spectrometry [11,12]. In analogy to other dynamical methods, e.g. dynamic-mechanical and dielectric experiments, the techniques use the modulation frequency as a variable parameter, now determining the dynamic heat capacity as a complex and frequency-dependent response function

$$c_p^*(\omega) = c_p'(\omega) - \mathrm{i}c_p''(\omega) = |c_p^*|\mathrm{e}^{-\mathrm{i}\varphi_c} \tag{1}$$

Due to the diffusive character of heat conduction, a periodic heat flux homogeneously absorbed at the surface of a plate like sample produces plane thermal waves with a wavelength λ which in the normal case of a real heat capacity is given by (see Eq. (18))

$$\lambda = \sqrt{\frac{8\pi^2\kappa}{\rho c_p \omega}} \tag{2}$$

* Corresponding author. Tel.: +49-761-203-5887; fax: +49-761-203-5855.
E-mail address: strobl@uni-freiburg.de (G. Strobl).

0040-6031/01/$ – see front matter
PII: S0040-6031(01)00551-2

Here κ is the heat conductivity and ρ the density of the sample. Depending on the thickness of the sample and the modulation frequency one finds two limiting cases. First, if the thermal wavelength is much larger than the sample thickness, we have the condition of the quasi-static calorimeter. In this case the temperature distribution is homogeneous and one determines the heat capacity of the material. This principle is represented by the TMDSC and the ACC technique. On the other hand, if the thermal wavelength is in the same order or smaller than the sample thickness, a temperature distribution arises and one observes a diffusive propagation of thermal waves. In this diffusive case, one determines either the effusivity

$$\epsilon = \rho\kappa c_p \tag{3}$$

or the diffusivity

$$D = \frac{\kappa}{\rho c_p} \tag{4}$$

by applying the 3ω-method or TTS, respectively.

For a complex dynamic heat capacity, the effusivity and the diffusivity become frequency-dependent and complex as well, and we have to write

$$\epsilon^*(\omega) = \epsilon'(\omega) - \mathrm{i}\epsilon''(\omega) = |\epsilon^*|\mathrm{e}^{-\mathrm{i}\varphi_\epsilon} \tag{5}$$

and

$$D^*(\omega) = D'(\omega) + \mathrm{i}D'(\omega) = |D^*|\mathrm{e}^{\mathrm{i}\varphi_D} \tag{6}$$

From the measurement of both $\epsilon^*(\omega)$ and $D^*(\omega)$, one can find again the heat capacity and thermal conductivity, as

$$c_p^*(\omega) = \frac{1}{\rho}\sqrt{\frac{\epsilon^*(\omega)}{D^*(\omega)}} \tag{7}$$

$$\kappa^*(\omega) = \sqrt{\epsilon^*(\omega)D^*(\omega)} \tag{8}$$

In the following, we discuss an experimental setup which enables $\epsilon^*(\omega)$ and $D^*(\omega)$ to be determined over a large frequency range extending from 10^{-2} to 10^2 Hz.

We first formulate the physics of the experiments in mathematical terms. Then the experimental setup will be described. Subsequently we show calibration measurements which check the performance. Finally, we present as an example the results of a dynamical study of the surface melting in poly(ethylene oxide) (PEO).

2. Physical basis

We begin with the quasi-static condition. If the temperature is homogeneous within the sample, an oscillating heating power of the form

$$P^*(t) = \overline{P} + \delta P_0 \mathrm{e}^{\mathrm{i}\omega t} \tag{9}$$

applied to a sample produces a temperature varying with the same frequency

$$T^*(t) = \overline{T} + \delta T^*(t) = \overline{T} + \delta T_0^* \mathrm{e}^{\mathrm{i}\omega t} \tag{10}$$

The oscillating parts are related by

$$mc_p^* \frac{\mathrm{d}}{\mathrm{d}t}\delta T^*(t) = \delta P_0 \mathrm{e}^{\mathrm{i}\omega t} \tag{11}$$

which leads to

$$c_p^*(\omega) = \frac{\delta P_0}{m\omega\delta T_0^*}\mathrm{e}^{-\mathrm{i}(\pi/2)} \tag{12}$$

In the diffusive case, we consider thermal waves of the form

$$\delta T^*(z,t) = \delta T_0^* \mathrm{e}^{\mathrm{i}(\omega t - k^* z)} \tag{13}$$

Both the real and the imaginary part of the complex wave vector

$$k^* = k' + \mathrm{i}k'' \tag{14}$$

are parallel to the z-direction. By inserting the expression into the temperature diffusion equation

$$\frac{\partial}{\partial t}\delta T^*(z,t) = \frac{\kappa}{\rho c_p}\frac{\partial^2}{\partial z^2}\delta T^*(z,t) = D\frac{\partial^2}{\partial z^2}\delta T^*(z,t) \tag{15}$$

we obtain the dispersion relation for thermal waves

$$\omega(k^*) = \mathrm{i}D(k^*)^2 \tag{16}$$

or reversely

$$k^*(\omega) = \sqrt{\frac{-\mathrm{i}\omega}{D}} = \sqrt{\frac{\omega}{D}}\mathrm{e}^{-\mathrm{i}(\pi/4)} \tag{17}$$

For a real diffusivity then both the real and the imaginary part of the wave vector have the same value with different signs

$$k' = -k'' = \sqrt{\frac{\omega}{2D}} \tag{18}$$

We discuss the situation where the sample is infinitely extended in z-direction with the surface at $z = 0$. If the oscillating part of the power with amplitude δP_0 is applied on a surface area S, it produces a heat flux component varying with the same frequency

$$j^*(z=0,t) = \frac{\delta P_0}{S}\,\mathrm{e}^{\mathrm{i}\omega t} \tag{19}$$

penetrating into the sample. Employing the heat conduction equation

$$j(z,t) = -\kappa\frac{\partial}{\partial z}T(z,t) \tag{20}$$

we obtain for the plane thermal waves at $z = 0$

$$\begin{aligned}\frac{\delta P_0}{S}\mathrm{e}^{i\omega t} &= -\kappa\frac{\partial}{\partial z}\delta T^* \quad (z=0,t)\\ &= \mathrm{i}\kappa k^*\delta T^*(z=0,t)\end{aligned} \tag{21}$$

and thus, for the temperature amplitude at the surface

$$\delta T_0^* = \frac{\delta P_0}{S}\frac{\mathrm{e}^{-\mathrm{i}(\pi/4)}}{\kappa\sqrt{\omega\rho c_p/\kappa}} = \frac{\delta P_0}{S}\frac{\mathrm{e}^{-\mathrm{i}(\pi/4)}}{\sqrt{\omega}\,\sqrt{\epsilon}} \tag{22}$$

If we insert this result and the dispersion relation into the expression for the thermal waves, we find

$$\delta T^*(z,t) = \frac{\delta P_0}{S}\frac{\mathrm{e}^{-\mathrm{i}(\pi/4)}}{\sqrt{\omega}\,\sqrt{\epsilon}}\,\mathrm{e}^{\mathrm{i}(\omega t-\sqrt{(\omega/2D)}z)}\,\mathrm{e}^{-\sqrt{(\omega/2D)}z} \tag{23}$$

Choosing appropriate experimental setups, it is possible to determine either the effusivity ϵ or the diffusivity D. If we measure the temperature oscillation on the surface of the sample, i.e. at $z = 0$, we obtain

$$\delta T^*(z=0,t) = \frac{\delta P_0}{S}\frac{\mathrm{e}^{-\mathrm{i}(\pi/4)}}{\sqrt{\omega}\sqrt{\epsilon}}\mathrm{e}^{\mathrm{i}\omega t} \tag{24}$$

The effusivity then follows as

$$\epsilon = \frac{\delta P_0^2}{S^2}\frac{1}{\omega|\delta T^*(z=0,t)|^2} \tag{25}$$

On the other hand, the temperature oscillation in the sample at $z = d$ is given by

$$\delta T^*(z=d,t) = \frac{\delta P_0}{S}\frac{\mathrm{e}^{-\mathrm{i}(\pi/4)}}{\sqrt{\omega}\,\sqrt{\epsilon}}\mathrm{e}^{\mathrm{i}(\omega t-\sqrt{(\omega/2D)}d)}\,\mathrm{e}^{-\sqrt{(\omega/2D)}d} \tag{26}$$

In this case, the diffusivity can be derived both from the phase and the attenuation of the thermal wave.

The given equations all refer to the usual case of a real dynamic specific heat, effusivity or diffusivity. The generalization to situations where these quantities are complex follows directly from corresponding replacements in the equations. Some special cases are dealt with later on.

3. Experimental setup

Measurements of the effusivity and the diffusivity are carried out with the same device, only the sample holder and the temperature sensor are different. The basic construction is shown in Fig. 1. Samples are heated by a light beam, whereby intensity modulations are produced by a chopper. The light is converted into heat by an optical absorber. The speed of the chopper determines the modulation frequency. The technical frequency range is 0.01–2500 Hz. In order to have a constant light intensity, part of the light beam is directed onto a photo diode using a beam splitter, and a PID-controller then keeps the intensity constant.

The temperature oscillations to be measured are converted into an ac voltage, in two different ways as described later. The voltage oscillations are measured by a lock-in amplifier which obtains the reference signal from the trigger of chopper. The averaging time used for one data point depends on the modulation period. It varies between 1500 s for the low frequencies and 300 s for the high frequencies. The amplifier measures both the amplitude and the phase of the voltage oscillations, which are proportional to the temperature oscillations.

Samples are introduced in a copper oven which is put into a dewar filled with liquid nitrogen. The oven can be heated electrically by a metal wire via a PID-controller and is cooled by the nitrogen atmosphere. The oven temperature can be varied from −100 to 200°C with a constancy of 0.1°C.

All experimental parameters, i.e. the oven temperature, the modulation frequency and the light intensity are controlled by a PC. At the same time the PC collects the measured data, in particular, the amplitude and phase of the temperature oscillations.

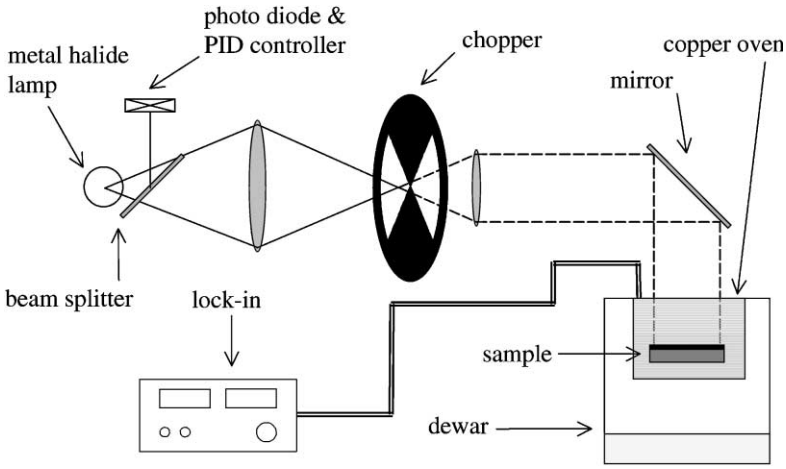

Fig. 1. Schematic of the basic experimental setup. The light intensity of a metal halide lamp is modulated by a mechanical chopper. An optical absorber transforms the light intensity into a thermal wave, which propagates through the sample. The phase and the amplitude of the thermal wave is measured by a lock-in amplifier, as described in the text. To keep the light intensity constant it is measured by a photo diode using a beam splitter, and a PID-controller then regulates the power supply of the light source.

3.1. Effusivity measurement

The sample holder used for the effusivity measurements is shown in Fig. 2. The sample is in a cylindrical form with a diameter of 30 mm and a thickness of 8 mm. The absorber is a graphite film, which is directly sprayed onto the sample surface.

The sensor for the detection of the thermal waves is a thermocouple which is fixed at the surface of the sample in direct contact with the absorbance layer. We use type E chromega/constantan thermocouples of 12 μm diameter supplied by Omega Engineering. The thermocouple junction is glued onto the sample surface with a small amount of epoxy resin.

For the measurement of the temperature oscillations, the thermocouple is connected to the lock-in amplifier via a high pass filter. The thermocouple is also used to measure the mean temperature at the

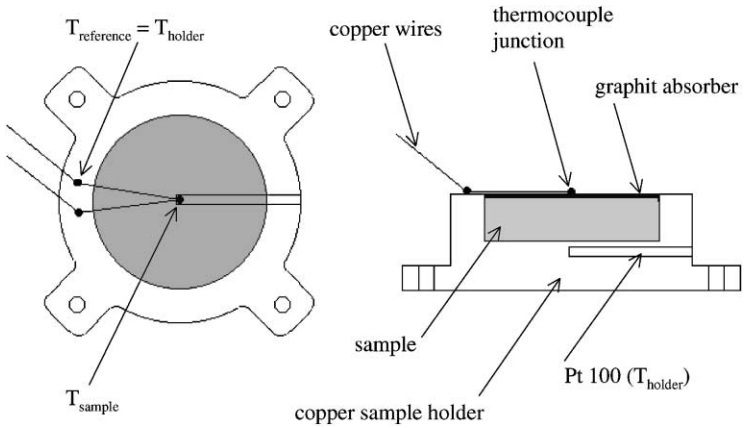

Fig. 2. Sample holder for effusivity measurements and attachment of the thermocouple temperature sensor. The reference junctions of the thermocouple are in contact with the sample holder.

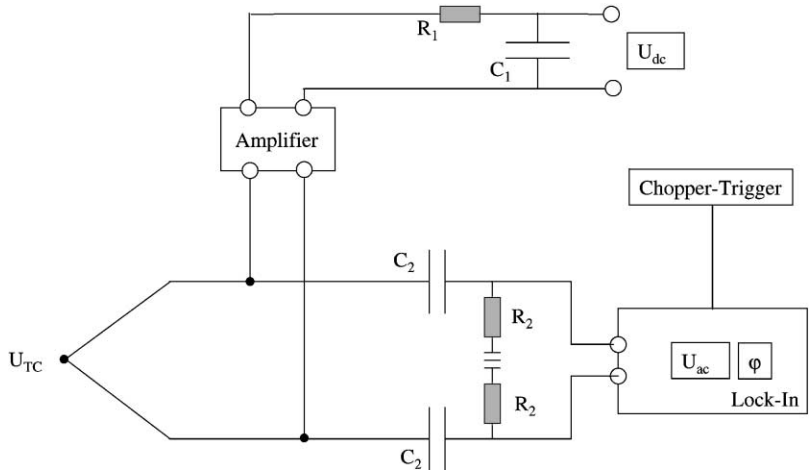

Fig. 3. Circuit diagram of the electronics for the effusivity measurement. To determine the dc part of the thermocouple voltage U_{TC}, it is connected to a low frequency amplifier and a following low pass filter ($R_1 = 1$ MΩ, $C_1 = 13.2$ μF). To determine the ac part, the thermocouple is connected to a lock-in amplifier via a high pass filter ($R_2 = 10$ MΩ, $C_2 = 4.7$ μF). The lock-in amplifier obtains the reference signal from the chopper-trigger.

sample surface. It is then connected to a low frequency amplifier (DLPVA-B from Femto Messtechnik GmbH) and a subsequent low pass filter, as shown in Fig. 3. The reference temperature at the connection points of the thermocouple wires and the copper wires leading out of the measuring cell is identical with the temperature of the sample holder. It is determined separately using a platinum resistor.

The thickness chosen for the samples in effusivity determinations has to be large enough to avoid a superposition of thermal waves reflected at the bottom of the sample.

The mathematical description of this setup corresponds to Eq. (24)

$$\delta T^*(z=0,t) = \frac{\delta P_0}{S\sqrt{\omega}} \frac{1}{\sqrt{\epsilon}} \mathrm{e}^{-\mathrm{i}(\pi/4)} \mathrm{e}^{\mathrm{i}\omega t}$$

If the heat capacity, the thermal conductivity and thus, the effusivity are real quantities, the amplitude δT_0 and the phase φ of the signal relative to the oscillation of the light are given by

$$\delta T_0 = \frac{\delta P_0}{S\sqrt{\omega}} \frac{1}{\sqrt{\epsilon}} \tag{27}$$

$$\varphi = -\tfrac{1}{4}\pi \tag{28}$$

In this situation the phase is constant and the thermal effusivity can be obtained from the amplitude. If there is an imaginary part in the heat capacity, the effusivity becomes a complex variable and the phase deviates from $-\pi/4$. Then we have

$$\delta T_0 = \frac{\delta P_0}{S\sqrt{\omega}} \frac{1}{\sqrt{|\epsilon^*|}} \tag{29}$$

$$\varphi = -\tfrac{1}{4}\pi + \tfrac{1}{2}\varphi_\epsilon \tag{30}$$

3.2. Diffusivity measurement

For diffusivity measurements we use the sample holder shown in Fig. 4. A sample of thickness d is placed between two glass slides (width: 26 mm, thickness: 10 mm, length: 76 mm). The upper glass slide is covered on the lower side with an optical absorber. The absorber is a sputtered CrN-film. The transmission for light is below 1%, and the reflectivity about 50%, the remaining 50% of the light are converted into heat. A gold film is sputtered onto the upper side of the lower glass slide, using a mask which produces the pattern shown on the left side of Fig. 4. This gold film is a temperature-dependent resistor and acts as temperature sensor. The meandering part in the center covering 7 mm^2 is the sensitive area. As this sensitive area is comparatively small and placed away from the edges, perturbations of the planarity of the waves, as they are found near the edges, can be ignored.

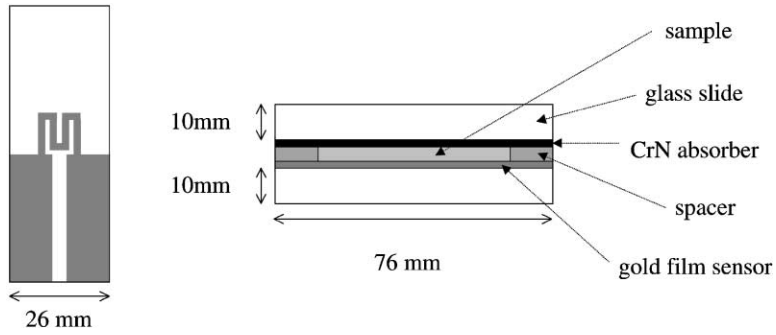

Fig. 4. Sample holder for diffusivity measurements (right) and gold film temperature sensor (left).

The thickness of the sample is fixed by kapton spacers. Different values were chosen for different ranges of the modulation frequency, thus, accounting for the changing attenuation. For the polymer sample, they are given in Table 1.

In order to measure temperature oscillations, the gold film resistor is connected to a constant current source as shown in Fig. 5. The ac part of the voltage is separated from the dc part by a high pass filter with a cut-off frequency of 0.0019 Hz. This frequency has been determined experimentally, and the necessary corrections for low frequencies were carried out numerically. The ac part of the signal is measured by a lock-in amplifier (SR830 from Standford Research).

The mathematical description of the setup requires a slight modification of Eq. (26), due to two features.

- The thermal wave initiated at the interface between the upper glass slide and the sample ($z = 0$) does not only propagate into the sample, but also into the glass.
- The thermal waves are partially reflected at the two interfaces at $z = 0$ and d.

Both factors lead to a reduction of the amplitude of the signal. For

$$\sqrt{\frac{\omega}{2D}}d > 1$$

one can neglect multiple reflections and account for the first reflection of the initiated wave only. A straightforward treatment shows that the reduced signal then is given by

$$\delta T^*(z=d,t) = \frac{\delta P_0}{S\sqrt{\omega}} \frac{1}{\sqrt{\epsilon}+\sqrt{\epsilon_G}} \frac{2\sqrt{\epsilon}}{\sqrt{\epsilon}+\sqrt{\epsilon_G}} e^{-i(\pi/4)} e^{i(\omega t - \sqrt{(\omega/2D)}d)} e^{-\sqrt{(\omega/2D)}d} \quad (31)$$

where ϵ_G is the effusivity of the glass substrate.

Table 1
Thicknesses of polymeric samples adapted to the different frequency ranges

Frequency range (Hz)	Sample thickness (μm)
0.01–2	375
1.5–9	110
5–110	55

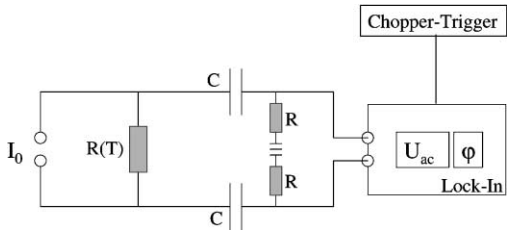

Fig. 5. Circuit diagram of the electronics for the diffusivity measurements. A constant current I_0 flows through the gold film which acts as a temperature-dependent resistor $R(T)$. With varying temperature the resistance changes and so does the voltage drop. The ac part of the voltage is separated from the dc part by a high pass filter ($R = 10\,M\Omega$, $C = 4.7\,\mu F$) and measured by a lock-in amplifier, which obtains the reference signal from the chopper-trigger.

In case there is no imaginary part in the heat capacity, and thus, no imaginary part in the diffusivity, the amplitude δT_0 and the phase φ of the temperature oscillation at $z = d$ relative to the oscillation of the light are

$$\delta T_0 = \frac{\delta P_0}{S} \frac{1}{\sqrt{\omega}} \frac{2\sqrt{\epsilon}}{(\sqrt{\epsilon} + \sqrt{\epsilon_G})^2} e^{-\sqrt{(\omega/2D)}\, d} \quad (32)$$

$$\varphi = -\frac{\pi}{4} - \sqrt{\frac{\omega}{2D}}\, d \quad (33)$$

In this case, the diffusivity D can be derived from the phase only. In the general case of a complex diffusivity we have, according to Eq. (16)

$$k^* = \sqrt{\frac{\omega}{D^*}}\, e^{-i(\pi/4)} = \sqrt{\frac{\omega}{|D^*|}}\, e^{-i((\pi/4)+(\varphi_D/2))} \quad (34)$$

The phase difference between the temperature oscillation at $z = d$ and the oscillating light intensity then follows as

$$\varphi = -\tfrac{1}{4}\pi - \tfrac{1}{2}\varphi_\epsilon - k'd \quad (35)$$

$$\varphi = -\frac{\pi}{4} - \frac{\varphi}{2_\epsilon} - \sqrt{\frac{\omega}{|D^*|}} \cos\left(\frac{\pi}{4} + \frac{\varphi}{2_D}\right) d \quad (36)$$

The term $-\varphi_\epsilon/2$ is due to the fact that

$$|\epsilon^*| \ll \epsilon_G \quad (37)$$

and therefore

$$(\sqrt{\epsilon^*} + \sqrt{\epsilon_G})^2 \approx \epsilon_G \quad (38)$$

Then the additional phase lag arising from the term $\sqrt{\epsilon^*}$ in Eq. (32) is given in good approximation by $-\varphi_\epsilon/2$. The expression for the amplitude is more complicated and, as it will not be used, not given here.

4. Performance checks

The properties of the temperature sensors were first checked by frequency-and temperature-dependent measurements using the glass slides only, i.e. without a sample.

For an examination of the gold film sensor we used a glass slide with a thin absorbing graphite layer on top of the sensor. The expected frequency dependence of the amplitude and the phase now is that of the effusivity measurement: the amplitude should be inversely proportional to the square root of the frequency ($\delta T_0 \sim 1/\sqrt{\omega}$) and the phase should constantly be at $-45°$. Fig. 6 shows the frequency-dependent measurement of the phase and the amplitude of the temperature oscillations. In the available frequency range, the result is close to the expected behavior.

The same measurement carried out with the thermocouple sensor yielded a similar result. It is shown in

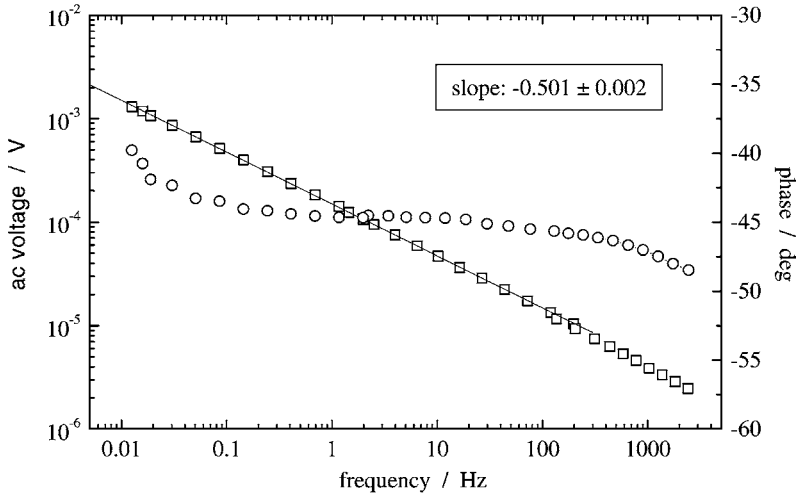

Fig. 6. Checking the performance of the gold film sensor. Signal measured if the absorbing graphite film is placed on top of the sensor on the same surface of the glass plate. Frequency dependencies of the ac-voltage proportional to the temperature amplitude and of the phase shift between light intensity and temperature.

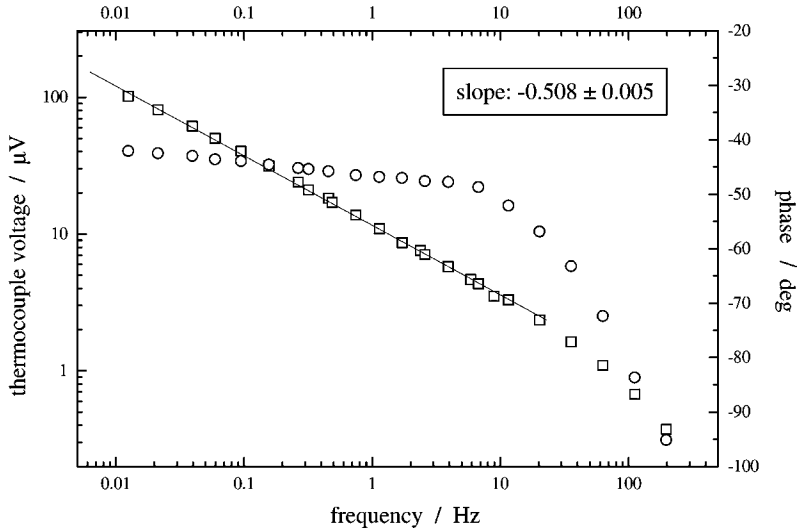

Fig. 7. Same experiment as in Fig. 6 now carried out for the thermocouple sensor.

Fig. 7. Here, the usable frequency range is smaller, due to the higher mass of the thermocouples, but within this range the behavior is again satisfactory. If necessary one could correct the damping of the amplitude and shifting of the phase with a low pass filter model.

In order to check the linearity with temperature of the gold film resistor the dc part of the experimental voltage was measured as a function of the temperature set in the oven. The sensor indeed shows a linear temperature dependence, as can be seen in Fig. 8.

5. An application: surface melting of PEO

As an example we present here the results of a study of the dynamics of surface melting in PEO [13,14].

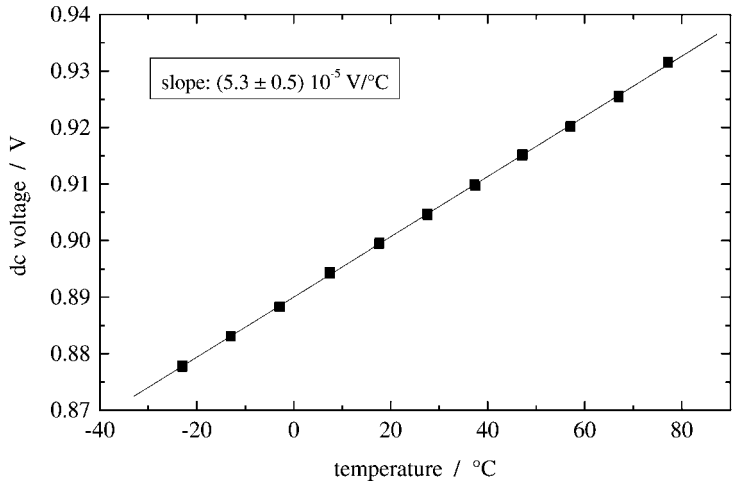

Fig. 8. Temperature dependence of the resistance of the gold film sensor, observed in a measurement of the voltage drop for a constant imposed current. The temperature coefficient is constant over a wide temperature range.

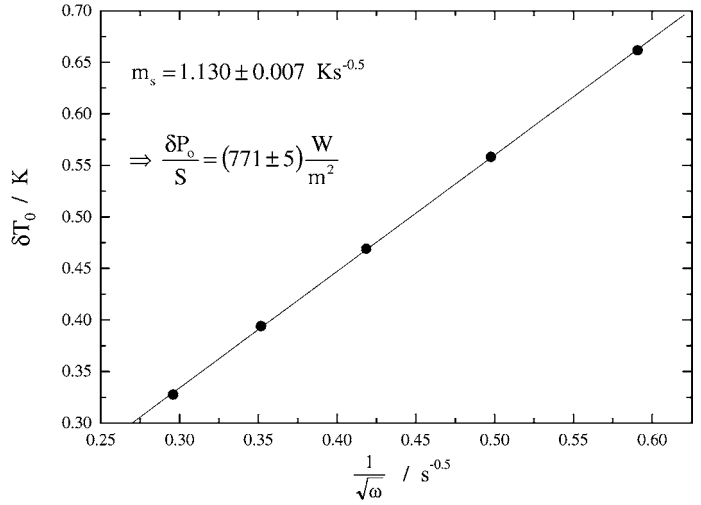

Fig. 9. Determination of the power δP_0 of the incident light. Knowledge of δP_0 is necessary for the data evaluation in effusivity measurements. The power can be deduced from the frequency dependence of the temperature oscillation amplitude δT_0.

Samples were purchased from Aldrich Chemical Company, Milwaukee, USA and Polysciences, Warrington, UK. Molecular weights were similar, $M_w \approx 300{,}000$ for both. Both samples included also amorphous silicon dioxide and calcium carbonate as additional ingredients. Samples were isothermally crystallized at 48°C, and then cooled to room temperature.

5.1. Effusivities

To determine the effusivity of the sample as a function of the mean temperature and the frequency, the amplitude and phase of the signal were measured at the top, in direct contact with the absorbance layer as described in Section 3.1. With Eq. (29) one obtains the modulus

$$|\epsilon^*(\omega)| = \left(\frac{\delta P_0}{S\sqrt{\omega}}\frac{1}{\delta T_0(\omega)}\right)^2 \tag{39}$$

and with Eq. (30) the phase of the effusivity of the sample.

As a prerequisite the value of $\delta P_0/S$ has to be known. There are different ways to determine it. First, it can be obtained by using the $1/\sqrt{\omega}$ frequency dependence of the temperature amplitude in Eq. (27) for temperatures in the melt region, where ϵ is real and frequency-independent and known from literature values for ρ, κ and c_p. In a plot of $\delta T_0(\omega)$ versus $1/\sqrt{\omega}$ as shown in Fig. 9 a linear fit results in a slope m_s, which is equal to $\delta P_0/(S\sqrt{\epsilon})$ according to Eq. (27). $\delta P_0/S$ follows from the slope as

$$\frac{\delta P_0}{S} = m_s \sqrt{\rho\kappa c_p} \tag{40}$$

Another possibility to determine this quantity is to measure the temperature gradient over the sample. The heat conductance equation, when applied to the mean values $\overline{T}$ and $\overline{P}$ reads

$$j = \frac{\overline{P}}{S} = -\kappa \,\mathrm{grad}\,\overline{T} \tag{41}$$

The chopper creates a rectangular light modulation with an amplitude

$$\Delta P = \overline{P} \tag{42}$$

The lock-in amplifier measures the first harmonic of the oscillating quantities. Taking into account the first order Fourier coefficient of a rectangular oscillation one obtains the relation between $(\delta P_0/S)$ and $\overline{P}$

$$\frac{\delta P_0}{S} = \frac{4}{\pi}\frac{\Delta P_0}{S} = \frac{4}{\pi}\frac{\overline{P}}{S} \tag{43}$$

Fig. 10 depicts as the result of a temperature-dependent measurement at a fixed frequency, $\nu = 0.6$ Hz, the modulus and phase of the effusivity.

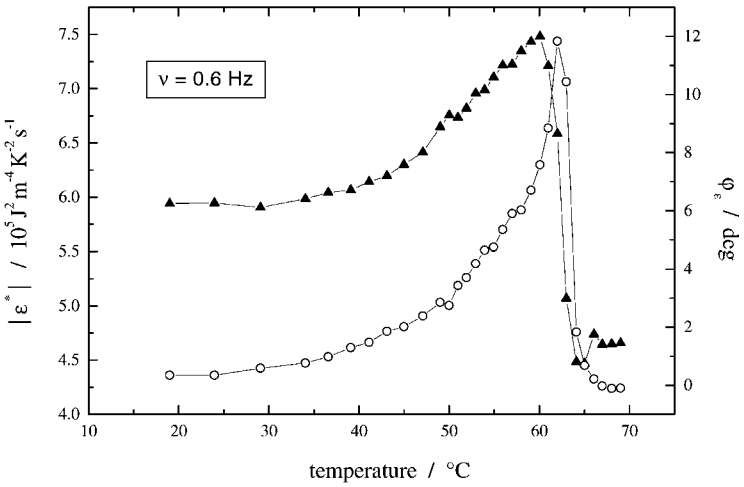

Fig. 10. PEO: temperature-dependent measurement at 0.6 Hz. Modulus (filled triangles) and phase (open circles) of the complex effusivity.

There is a prominent peak in the melting region below 63°C. This peak can be attributed to the reversible surface melting of PEO, as has been indicated by Hu et al. [15] and will be explained in more detail in another paper [16]. The result demonstrates also, that its appearance is accompanied by a non-vanishing phase angle φ_ϵ. Most interestingly, the peak height is dependent on the modulation frequency. This is shown by Fig. 11 which presents the temperature dependence of $|\epsilon^*|$ for different frequencies. We can conclude from this observation that the period of the modulation is obviously in the same range as the characteristic time associated with the surface melting.

5.2. Diffusivities

First we measured the diffusivity in the molten state at 72°C, where D is a real, frequency-independent quantity. D can be determined in absolute values by a

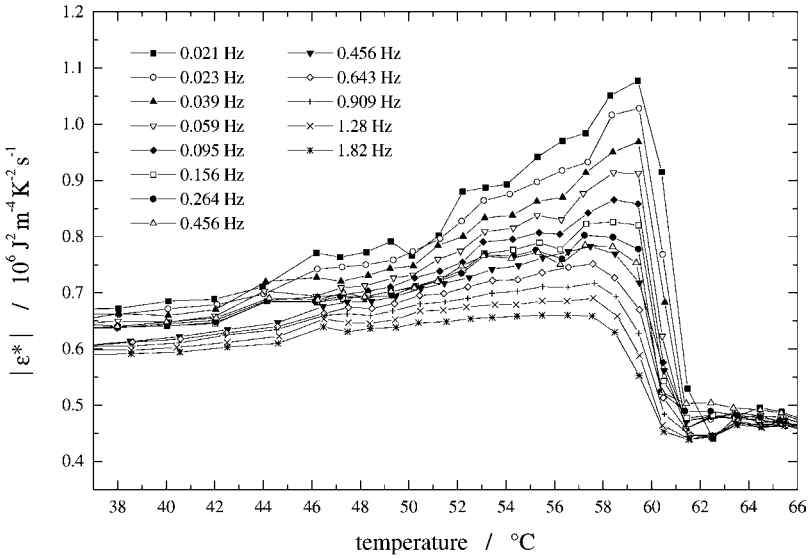

Fig. 11. Frequency and temperature dependence of the effusivity of PEO in the melting region.

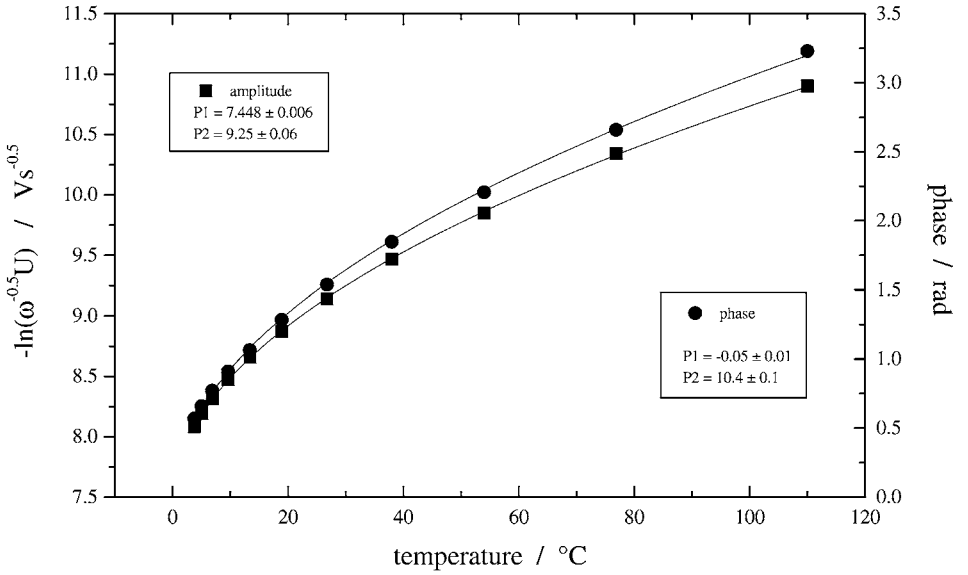

Fig. 12. Derivation of the diffusivity of molten PEO (72°C) from frequency dependent measurements. Fits for the ac-voltage (proportional to δT_0) and the phase based on Eq. (44), resulting in the indicated values of P_1 and P_2.

frequency-dependent measurement of the phase and the amplitude of the temperature oscillation at the bottom of the sample. According to Eqs. (32) and (33), both the phase φ and the expression $\ln(\sqrt{v}\,\delta T_0)(\omega = 2\pi v)$, which includes the amplitude δT_0, are given by a function of the form

$$f(v; P_1, P_2) = P_1 - \sqrt{\frac{v}{P_2}} \quad (\omega = 2\pi v) \tag{44}$$

The parameter P_2 is proportional to the diffusivity.

$$P_2 = \frac{D}{(d^2\pi)} \tag{45}$$

Fig. 12 shows the phase and the amplitude as a function of the modulation frequency for a liquid PEO sample with a thickness of 55 μm in the frequency range between 2 and 110 Hz together with the respective fits. All results obtained in this way for different sample thicknesses in the corresponding frequency ranges are shown in Table 2, together with the diffusivity values derived from P_2.

The value for the diffusivity of liquid PEO averaged over the three samples, as derived from both the phase and the amplitude, is $D = (8.9 \pm 0.6) \times 10^{-8}$ m^2 s^{-1}. In the literature one finds [17], $D = 9.0 \times 10^{-8}$ m^2 s^{-1}. The agreement is quite good. Thus, we are able to determine absolute values for the diffusivity of polymeric materials.

In the next step, we determined the diffusivity of PEO as a function of temperature and frequency in the melting region of PEO. The result is shown in Fig. 13. The findings for the (reciprocal) diffusivity obviously agree with those for the effusivity. Again a peak shows up in the melting range, and its height decreases with increasing frequency. The dependence is shown in Fig. 14. We, thus, have further confirmation, that the surface melting in PEO takes place on time scales in the range probed by our experiments.

The data in Fig. 13 were obtained applying Eq. (33), i.e. under neglect of the non-vanishing phase angle φ_D. This is possible considering the results of the effusivity measurements. The changes in the measured

Table 2
Diffusivities of liquid PEO at 72°C, derived from measurements in different frequency ranges

Frequency (Hz)	d (μm)	P_2 (Hz) from ampliude	P_2 (Hz) from phase	D (10^{-8} m^2 s^{-1})
0.012–0.5	375	0.17	0.2	8.2
0.35–8.8	110	2.1	2.7	9.1
4–150	55	10.45	9.35	9.4

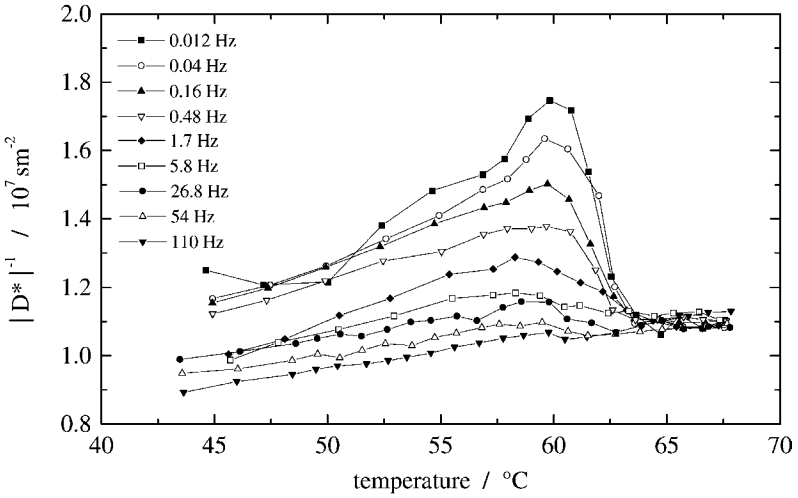

Fig. 13. Frequency and temperature dependence of the reciprocal diffusivity of PEO in the melting region.

phase delay φ through the melting range caused by the surface melting were large compared to φ_ϵ. Eq. (36) indicates that, assuming $\varphi_\epsilon \simeq \varphi_D$, the effect of the imaginary component then is indeed small.

5.3. Derivation of the heat capacity and conductivity

With the knowledge of the diffusivity and the effusivity one can now derive the heat capacity and the thermal conductivity in dependence on temperature and frequency, employing Eqs. (7) and (8). We chose the value $\rho = 1.13\ \mathrm{g\,cm^{-3}}$ for the density of PEO, as given in the literature [17].

The values, thus, obtained for the modulus of the heat capacity and the thermal conductivity are shown in Figs. 15 and 16. The results demonstrate that the peaks in the reciprocal diffusivity and the effusivity are due to a corresponding peak in the heat

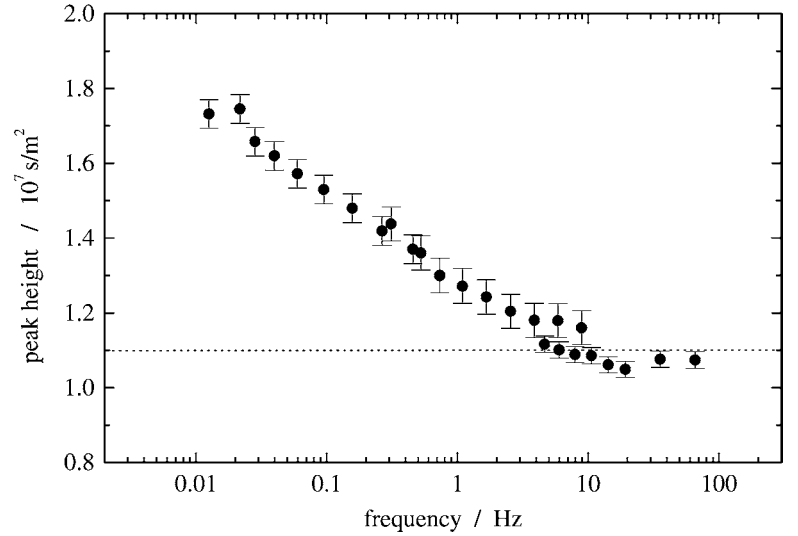

Fig. 14. Height of the peak in Fig. 13 vs. frequency.

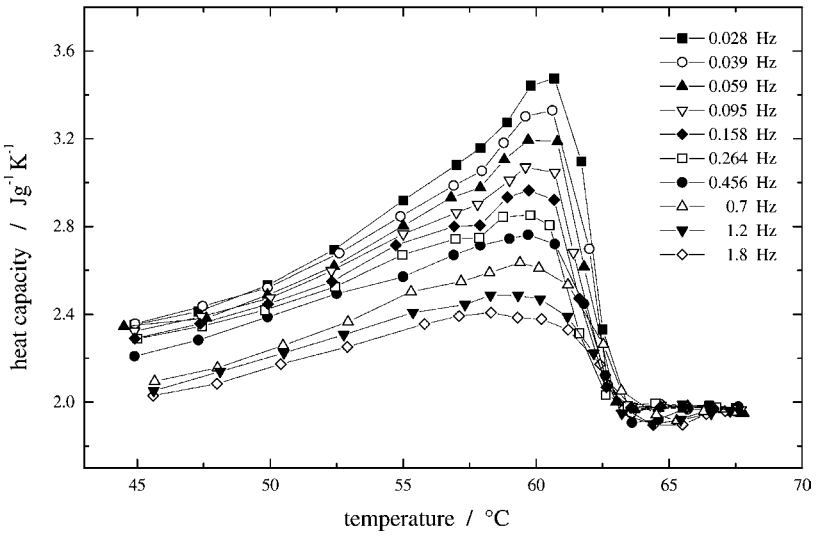

Fig. 15. PEO: temperature dependence of the modulus of the complex heat capacity, deduced from the measured diffusivity and effusivity.

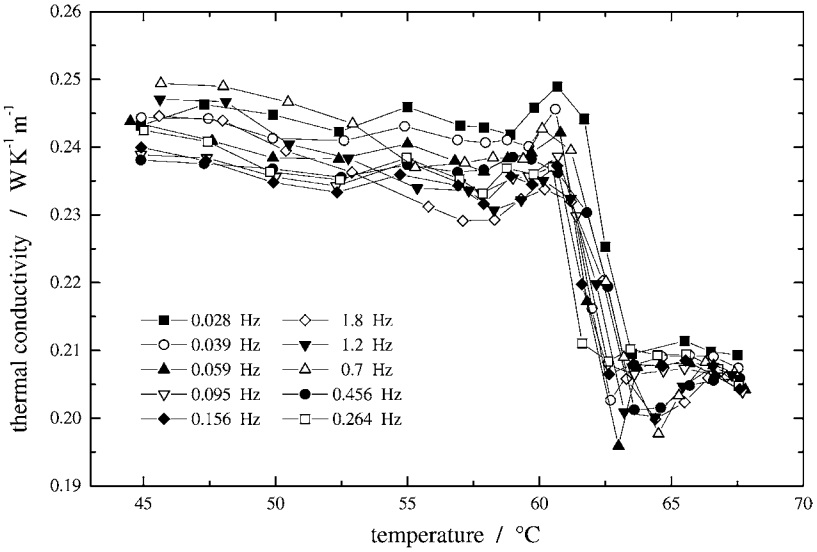

Fig. 16. PEO: temperature dependence of the thermal conductivity, deduced from the measured diffusivity and effusivity.

capacity, with the same frequency dependence. The thermal conductivity shows in the melting region only a step-like decrease. It is related to the irreversible melting of the crystal lamellae, i.e. to the decrease of the crystallinity down to zero. Within the error limits of the data, there is no indication for a frequency dependence.

6. Conclusions

A new modulated light calorimeter has been developed, working in the diffusive region. The calorimeter can be operated in two different modes, to be used in measurements of the effusivity or the diffusivity of a sample, respectively. The accessible frequency range

is four magnitudes large, extending from 0.01 up to 100 Hz. The temperature fluctuations of the oven are below 10 mK.

Measurements carried out for PEO show that the new calorimeter can be successfully applied to study the thermal properties of polymers at frequencies up to 100 Hz. The expected effect of reversible surface melting has been observed and the related characteristic dynamical time could be measured.

The combination of diffusivity and effusivity data was used to deduce both the heat capacity and the thermal conductivity.

Acknowledgements

Support of this work by the Deutsche Forschungsgemeinschaft (Sonderforschungsbereich 428, Freiburg) is gratefully acknowledged.

References

[1] M. Reading, Trends Polym. Sci. 8 (1993) 248.
[2] B. Wunderlich, A. Boller, I. Okazaki, K. Ishikiriyama, W. Chen, M. Pyda, J. Pak, I. Moon, R. Androsch, Thermochim. Acta 330 (1999) 21–38.
[3] J.M. Hutchinson, Thermochim. Acta 324 (1998) 165–174.
[4] A. Toda, Y. Saruyama, Polymer 38 (11) (1997) 2849–2852.
[5] I. Hatta, Thermochim. Acta 305 (1997) 27–34.
[6] K. Ema, T. Uematsu, A. Sugata, H. Yao, Jpn. J. Appl. Phys. 32 (1993) 1846–1850.
[7] N.J. Garfield, M.A. Howson, N. Overend, Rev. Sci. Instrum. 69 (1998) 2045–2049.
[8] A.A. Minakov, C. Schick, Thermochim. Acta 330 (1999) 109–119.
[9] A.A. Minakov, Y.V. Bugoslavsky, C. Schick, Thermochim. Acta 317 (1998) 117–131.
[10] T. Hashimoto, J. Morikawa, T. Kurihara, T. Tsuji, Thermochim. Acta 304/305 (1997) 151–156.
[11] N.O. Birge, S.R. Nagel, Rev. Sci. Instrum. 58 (1987) 1464.
[12] N.O. Birge, P.K. Dixon, N. Menon, Thermochim. Acta 304/305 (1997) 51–56.
[13] G. Strobl, The Physics of Polymers, Springer, Berlin, 1997, p. 185.
[14] T. Albrecht, G. Strobl, Macromolecules 28 (1995) 5827–5833.
[15] W.B. Hu, T. Albrecht, G. Strobl, Macromolecules 32 (22) (1999) 7548–7554.
[16] T. Albrecht, S. Armbruster, S. Keller, G. Strobl, Macromolecules, submitted for publication.
[17] D.W. van Krevelen, Properties of Polymers, Elsevier, Amsterdam, 1976, p. 576